LIDAR MONITORING OF THE NEAR-SURFACE ATMOSPHERIC AEROSOL CONTENT OVER SOFIA URBAN ZONES

Tanja Dreischuh, Zahari Peshev, Ivan Grigorov, Ljuan Gurdev, Atanaska Deleva, Georgi Kolarov, Dimitar Stoyanov

Institute of Electronics – Bulgarian Academy of Sciences
e-mail: tanjad@ie.bas.bg

Keywords: *Aerosol, lidar, scanning lidar, near-surface aerosol lidar mapping, air-quality monitoring*

Abstract: *In this paper, recent experimental results are described and analyzed, concerning the distribution of the aerosol load in the near-surface atmospheric layer above Sofia City. The measurements were performed at the Laser Radar Laboratory of the Institute of Electronics of the Bulgarian Academy of Sciences using laboratory Light Detection And Ranging facilities (LIDARs). Urban and suburban areas were examined, located near and far from sources of air pollution of different aerosol types. The results obtained are presented as polar diagrams of the aerosol backscattering coefficient distribution superimposed on the map of Sofia City region. In addition, color maps in range-time coordinates are also displayed and analyzed, showing the temporal dynamics of the near-surface aerosol density distribution along fixed lidar-measurement directions crossing the investigated areas. In some of the regarded cases, the lidar backscattering coefficient data obtained are calibrated using data of in-situ measurements, allowing one to determine the spatial distribution of the aerosol mass concentration and the zones where it exceeds the permissible limit values. Expectedly, we found that the aerosol mass concentration reaches maximum values near industrial sources of pollutants and over heavy-traffic zones. The results might be of importance to the city authorities, providing them with fast and range-resolved information about air pollution levels over broad urban areas.*

ЛИДАРЕН МОНИТОРИНГ НА ПРИЗЕМНИЯ АЕРОЗОЛЕН СЪСТАВ НА АТМОСФЕРАТА НАД СОФИЯ

Таня Драйшу, Захари Пешев, Иван Григоров, Люан Гърдев, Атанаска Делева, Георги Коларов, Димитър Стоянов

Институт по електроника – Българска академия на науките
e-mail: tanjad@ie.bas.bg

Ключови думи: *Аерозол, лидар, сканиращ лидар, лидарно картографиране на приземните атмосферни слоеве, контрол на атмосферните замърсявания*

Резюме: *В работата са описани и анализирани някои последни експериментални резултати относно разпределението на аерозолната натовареност в приземния атмосферен слой на град София. Измерванията са извършени от екип на лаборатория „Лазерна Локация" на Института по Електроника към Българската Академия на Науките, използувайки лидарните установки на лабораторията. Изследвани са градски и извънградски зони, разположени в близост до или отдалечени от източници на различни аерозолни замърсявания. Получените резултати са изобразени като полярни диаграми на разпределението на аерозолния коефициент на обратно разсейване, разположени върху географски карти на района на София. Представени и анализирани са, също така, и цветови карти в координати разстояние-време, показващи динамиката на разпределението на плътността на приземните аерозолни слоеве по фиксирано направление, пресичащо изследваните области. За някои от разгледаните случаи, получените стойности на коефициента на обратно разсейване са калибрирани по отношение на аерозолната масова концентрация, което позволява да се определят пространственото разпределение на последната, както и зоните, където тя надвишава пределно допустимите стойности. Установено е, както може да се очаква, че масовата концентрация е максимална в близост до индустриални източници на замърсявания или оживени пътни артерии или кръстовища. Резултати, подобни на тези, получени в настоящата работа, са от особено значение за градските власти, предоставяйки им своевременно и с висока разделителна способност информация за нивата на замърсяване на въздуха в обширни райони.*

Introduction

Earth's atmosphere contains an immense amount of aerosol particles, known also as particulate matter (PM). Atmospheric aerosols are of primary importance for the energy exchange between the Sun and the Earth, influencing heavily the climate and living conditions on Earth [1]. The near-surface aerosol particles may have an even stronger direct negative effect on the ecosystems and the human health [2 and references therein]. Penetrating into the human's respiratory tract, they can be extremely harmful, causing various mechanical, chemical, radiological and microbiological impacts [3]. The fine and ultrafine aerosol particles, sized in the micron and submicron range, are especially dangerous in this case, because they are hardly removable by the organism. Therefore, the near-surface atmospheric aerosol load is of crucial importance for the quality of life. By monitoring this load, information could be derived about the concentration and nature of the aerosol pollutions, as well as about the actions to be undertaken by the city authorities to diminish their negative effects.

The LIght Detection And Ranging systems (LIDARs) are the most appropriate instruments for express monitoring on a vast scale and with a high spatial resolution of the distribution and nature of the aerosol particulate matter in the atmosphere as a whole and in its near-surface layer, in particular [4, 5]. Lidar scanning of the near-surface (living) atmospheric layer along with the contact *in-situ* monitoring by ecological stations provides valuable information about the local density, spatial distribution, and temporal dynamics of polluting aerosol loads over broad areas. Such information allows one to timely warn the city authorities of arising health hazard. This is why the near-surface aerosol field has long been a subject of particular attention for the Laser Radar Laboratory of the Institute of Electronics of the Bulgarian Academy of Sciences (LRL-IE) [6]. In this respect, the main purpose of the present work is to describe and discuss some results obtained recently concerning the distribution of particulate matter in the atmospheric layer near the Earth surface in Sofia City region.

In the following Section we briefly describe the lidar facilities employed and the methods of extracting (from the lidar data) the information about the aerosol extinction and backscattering coefficients and mass concentration. Then, the main results obtained in the work are presented and analyzed. In the last Section, the main conclusions are summarized.

Experimental instruments and methods

Lidar systems and observation zones

The measurements were conducted by horizontal scanning of observation zones over Sofia using lidar systems developed at the LRL-IE [6]. They are of the monostatic non-coaxial type. The first of them (Fig. 1a) has an elastic and a Raman receiving channels, the former being in use in this work. The light transmitter in this system is a frequency-doubled Nd:YAG laser with a pulse energy of up to 600 mJ at λ = 1064 nm and 80 mJ at λ = 532 nm, a pulse repetition rate of 2 Hz, a pulse duration of 15 ns, and a beam divergence of 2 mrad. The receiving optics consists of a Cassegrain-type telescope with an aperture of 35 cm, a focal distance of 200 cm, and a three-channel wavelength separator comprising dichroic beam splitters and three 1–3 nm passband interference filters. The receiving electronic part consists of three compact electronic modules, each one including a 10 MHz 14-bit analog-to-digital converter (ADC), a high-voltage power supply, and controlling electronics. The backscattered lidar signals from the atmosphere are digitized every 100 ns by the ADC, which provides a range resolution of 15 m. The accessible range of this lidar is about 30 km. It is mounted on a stable metal coaxial construction allowing reliable fixing and precise synchronized mutual motion of both the telescope and the output laser beam in horizontal (toward Vitosha Mountain) and vertical direction with an angular resolution of about 1 degree.

The second system (Fig. 1b) is an elastic lidar, whose transmitting unit consists of a pulsed CuBr-vapor laser emitting at the wavelength λ = 510.6 nm and a beam-forming expander-collimator. The mean power and repetition rate of the emitted laser pulses are 2.5–3 W and 12 kHz, respectively. The pulse duration is 15 ns. The receiving optics comprises a Cassegrain-type telescope with an aperture diameter of about 0.2 m and a focal distance of 1 m, a 2-mm-wide focal diaphragm, and an interference filter with a 2-nm-wide passband. The angle of view of the receiving system is ~ 2 mrad. The backscattered laser light is detected in a photon-counting mode using EMI 9789 photomultipliers with a spatial resolution along the lidar line of sight (LOS) of 30 m and accumulation time of 5 minutes. The azimuthal and elevation angles of the LOS can be scanned with a step of 1 degree.

The lidar systems are installed, respectively, on the fourth floor and on the roof of the IE-BAS building (42.65 N, 23.38 E; 590 m a.s.l.), in the southeast part of Sofia. They are employed to perform lidar mapping experiments in the south-southwest and in the north-northwest directions, respectively. Thus, surface areas of about 100 km^2 are scanned and mapped over the central city zone, the north industrial zone and the south urban and suburban parts, including the north slopes of Vitosha Mountain,

allowing us to detect and analyze aerosols of different origin (natural, urban, industrial, etc.), with the aim of contributing to the establishment of a modern city air-quality monitoring system.

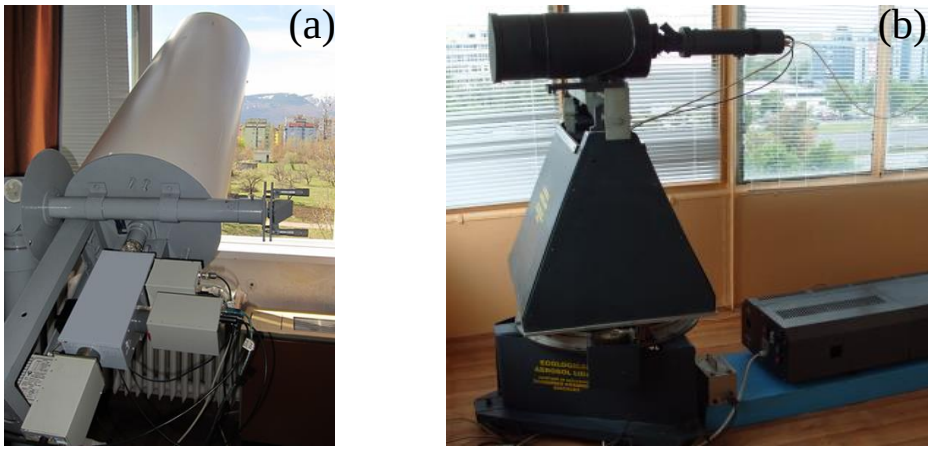

Fig. 1. Lidar systems based on a Nd:YAG laser transmitter (a) and a CuBr-vapor laser transmitter (b)

Determining the aerosol extinction and backscatter coefficients and mass concentration

The monostatic lidar sensing of the atmosphere requires pulsed laser radiation in order to ensure range-resolved detection of the laser light backscattered from the atmosphere. The temporally successive direct detection of the backscattered light, at the same wavelength as the sensing laser wavelength λ, produces a variable electrical (direct current or photon-counting-based) signal, called the lidar signal profile, which is a projection in time of the light-power portions arriving from successive elementary scattering volumes along the lidar LOS. The lidar profile, as a function of the lidar parameters and the LOS profiles of the atmospheric extinction $\sigma(r)$ and backscattering $\beta(r)$ coefficients, is described by the so-called lidar equation [7], whose solution with respect to $\sigma(r)$ and $\beta(r)$ is obtainable using the Klett-Fernald or the slope (logarithmic-derivative) approaches [7–9]; $r = ct/2$ is the coordinate along the LOS.

The first approach leads to a stable solution of the lidar equation and is being widely applied now. An inverse integration algorithm is used, starting from the far end of the lidar sounding path, where the aerosol backscatter coefficient is either negligible compared to the molecular backscatter coefficient or is known from other sources. In the case of molecular (Rayleigh) atmospheric scattering, the value of the so-called lidar ratio $S = S_m = \sigma_m(r)/\beta_m(r) = 8\pi/3$ is known [7]. Then, after measuring, e.g., by radiosondes, the vertical molecular density profile, or using the Standard Atmosphere Model [10] one could determine independently the molecular extinction $\sigma_m(r)$ and backscatter $\beta_m(r)$ profiles at wavelength λ. Their knowledge allows one to determine $\sigma_a(r)$ and $\beta_a(r)$ provided that the aerosol lidar ratio $S_a(r) = \sigma_a(r)/\beta_a(r)$ is known and invariant along the laser beam path [8, 9]. The exact value of this ratio is determined depending on the laser wavelength and also on *a priori* assumptions about the atmospheric conditions and the type of the aerosols observed. One may assume that near the ground $S_a \sim 40–60$ sr for hazy atmosphere and ~20–30 sr for clear atmosphere [11, 12].

In the case of horizontal or quasi-horizontal lidar sensing of the near-surface atmospheric layer, which is rich in aerosols so that molecular reference values of $\beta_m(r)$ could not be used, one can employ alternative approaches to solve the lidar equation in order to characterize the aerosol content in the observation areas. In such instances, there may exist LOS zones with relatively homogeneous aerosol composition and concentration providing conditions favorable for applying the slope (logarithmic-derivative) method. In the present experiments, a combination of the two methods described was used, whereby the slope method was applied to determining $\sigma_a(r)$ and $\beta_a(r)$ in appropriate parts of the lidar beam path, while the values of $\beta_a(r)$ thus obtained were used as reference ones in retrieving the whole range profiles of $\beta_a(r)$ by means of the Klett-Fernald approach. As a result, the range profiles of the aerosol extinction and backscatter coefficients were retrieved with relatively high precision and reliability; these were accordingly transferred to the color maps based on them of the near-surface aerosol density distribution.

The spatial distribution of the aerosol mass concentration C_m can be estimated by assuming that the mass concentration is proportional to the aerosol extinction and backscattering coefficients determined by the lidar. The corresponding coefficients of proportionality, K_σ and K_β, can be obtained as slopes of regression lines fitting the data from parallel lidar and contact measurements of the extinction and backscatter coefficients and the mass concentration, respectively (e.g., [13, 14]).

Results and discussion

Below we present and discuss recent results of lidar monitoring of the near-surface atmospheric aerosol content over Sofia City region obtained along a fixed direction or by horizontal scanning.

Fig. 2 shows results of a quasi-horizontal lidar scanning of the near-ground aerosol density carried out on Feb. 20, 2019 by using the Nd:YAG lidar's infrared spectral channel (wavelength of 1064 nm) at a slope angle of 6˚ and in a horizontal angular section of 50˚ to the south-southwest from the lidar station. The blank section is due to objects obstructing the laser beam. Fig. 2a is a color-coded diagram of the aerosol density spatial distribution in arbirary units; in Fig. 2b, this color map is superimposed over the map of the area allowing us to differentiate the characteristics of the aerosol pollution above the urban and suburban zones within the sector of lidar observation. This color map, with the specificities it illustrates, presents a typical aerosol distribution pattern that we consider as being representative for the results of our measurements of the aerosol pollution over the urban areas considered here. As one can see, the aerosol density is maximal (red-colored areas) over the densely populated *Mladost 1–4* residential districts, which are also characterized by thoroughfares with heavy traffic. The aerosol density remains moderately high (predominant yellow-orange coloration) up to Sofia city ring road; it decreases gradually above the suburban areas close to *Vitosha* Mountain, especially so over the mountain slopes (colored correspondingly in green-blue and blue).

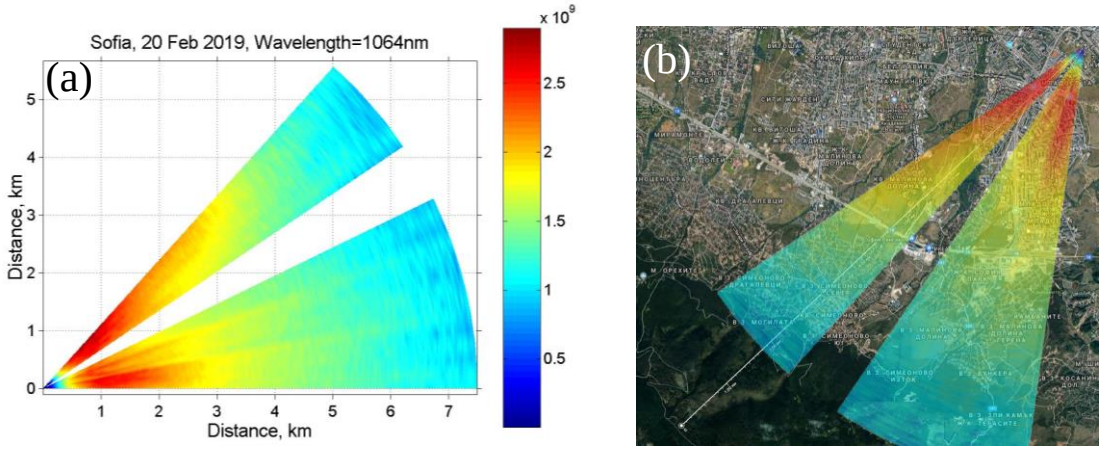

Fig. 2. Sectoral color maps of the aerosol density obtained by quasi-horizontal scanning by the Nd:YAG aerosol lidar in southwest direction: (a) color-coded diagram of the spatial aerosol distribution; (b) map of the area with the color map superimposed on it

Fig. 3 displays results from measurements of the aerosol density temporal development along a fixed southwest LOS carried out by the Nd:YAG aerosol lidar around midday on June 7, 2019. The infrared lidar channel was used (wavelength 1064 nm) at a slope angle of 4° with respect to the horizon. The aerosol pollution was thus observed over this particular urban area along the direction chosen, spreading up to the city ring road (distance of 4 km). Fig. 3a is a color-coded diagram of the aerosol density spatial-temporal distribution in arbirary units; in Fig. 3b, this color map is superimposed on the map of the area in order to follow the aerosol pollution dynamics above the selected sections of the urban zone located around the LOS. In contrast to the previous case of sector lidar scanning, in Fig. 3 the color map does not lie in the geographical map plane, but is rather projected only on the LOS (marked by a white line); the figure thus provides a convenient visual correlation of the dynamic aerosol pollution picture with the corresponding areas along the direction chosen. As seen, the LOS passes above two distinct characteristic zones. The first one is a typical urban zone comprising the densely populated *Mladost 1*, *Mladost 1A* and *Mladost 2* districts and extending to a distance of about 2.5 km from the lidar station. The second part of the lidar beam path traverses a park and a sparsely populated urban zone reaching 4 km away from the lidar in the ring road vicinity. Correspondingly, the two figure parts exhibit significantly differing aerosol densities. Over the heavily populated urban area near the lidar, one can see a noticeably higher aerosol concentration (yellow-red coloring), combined with a higher density distribution dynamics; while over the park zone most of the time the aerosol content is significantly lower (predominant blue-green and yellow coloring). Along with the systematically high aerosol density within the 0.3–1.3 km range, an interesting result is the "aerosol island" partially connected to the adjacent dense aerosol zones and detected in the middle of the measurement time interval at a distance of about 2 km. By the end of the measurement period, sections with higher aerosol densities can also be seen over the park area, which are probably due to air mass advection from the nearby zones of high aerosol content. In summary, the dynamic picture of the aerosol distribution

observed along the lidar LOS demonstrates the lidar technique's exceptional capabilities in detecting and characterizing aerosols in the near-ground atmospheric layer with high sensitivity and reactivity to the presence and variations of the aerosol pollutions in this layer.

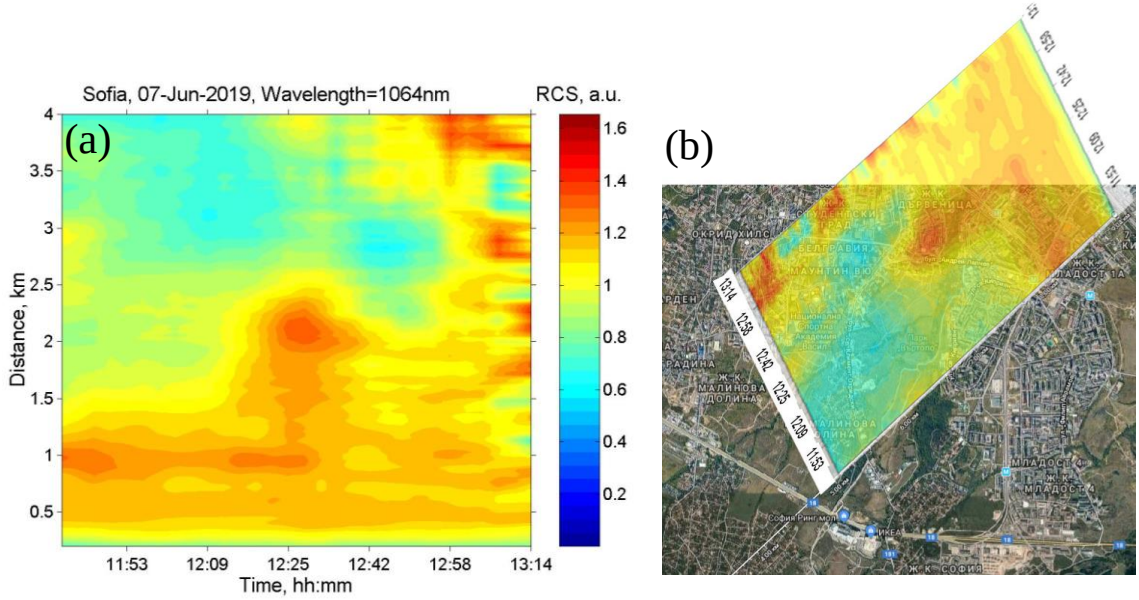

Fig. 3. Dynamic color map of the near-ground aerosol density obtained by quasi-horizontal sounding by the Nd:YAG aerosol lidar in a fixed southwest direction: (a) spatial-temporal color diagram; (b) dynamic color map superimposed on the map of the area along with the LOS (indicated by a white line)

Figs. 4 and 5 illustrate the results of our further recent experiments, namely, horizontal lidar sensing of the aerosol field at about 20–40 m above ground using the lidar system based on a CuBr vapor laser. Fig. 4 displays the results from the observation conducted on March 13, 2019, of the aerosol field evolution along a fixed LOS direction from the IE-BAS toward Droujba residential district. The signal-accumulation (sampling) time interval was 5 minutes. In Fig. 4a, the presence is clearly seen of a permanent high-intensity source of aerosol pollution (with high values of $\beta \sim 3.5 \times 10^{-3}$ km^{-1} sr^{-1}) at a distance of 7 km. Let us assume that $S_a = 50$ sr and $K_\sigma = 0.17$ km mg m^{-3} [14]. Then, the aerosol peak mass concentration at the 7-km distance will be $C_m \approx K_\sigma S_a \beta \approx 30$ μg m^{-3}, which is near the acceptable PM_{10} concentration threshold [15,16]. The color map from Fig. 4a imposed on the map of Sofia (district Droujba) shows (Fig. 4b) the location of the industrial source of PM pollution and its local small-size character. At other distances along the LOS one can observe other aerosol inhomogeneities with relatively smaller concentration and restricted lifetime or spatial scale. One may notice as well a low-concentration aerosol field given in yellow, extending from one to six kilometers along the LOS.

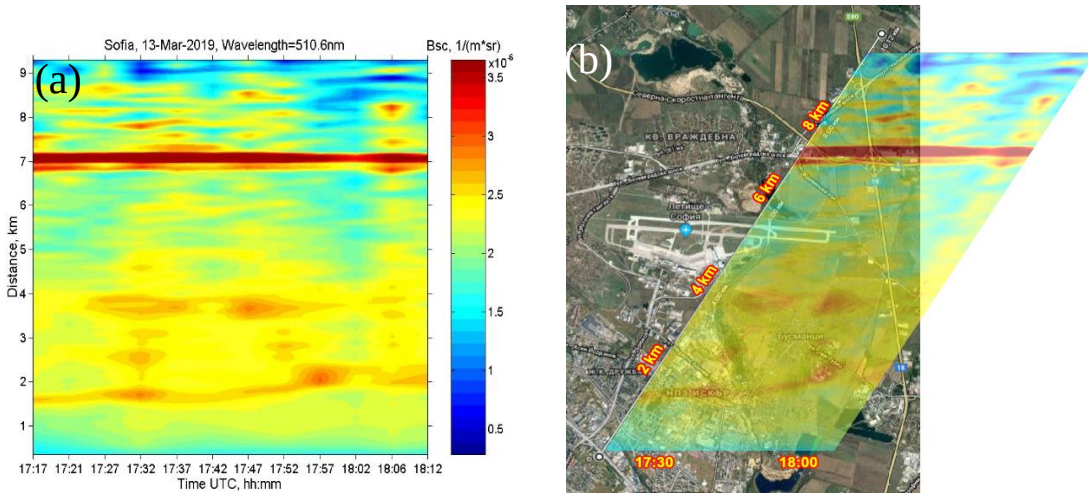

Fig. 4. Temporal evolution of the aerosol density distribution along a horizontal line of sight of the CuBr-laser-based lidar system, measured on 13 March 2019 (a) and superimposed on the map of Sofia (district *Droujba*) (b)

Fig. 5 is a horizontal scan of the LOS at a step of 1.6 degrees around the direction toward Sofia City center above Tsarigradsko Chaussee blvd. The experiments were conducted on April 8, 2019. The signal-averaging time at each angular position was 5 min. Zones with low (in blue) and high (in yellow and red) aerosol concentration are clearly seen in Fig. 5a. The color map superimposed on the map of Sofia shows that (Fig. 5b) the areas of high aerosol concentration are near the Tsarigradsko Chaussee blvd. and the crossing roads with heavy traffic. Thus, the results obtained by the lidar system confirm the expectation that the industrial facilities and the intensive traffic are the main sources of aerosol pollution in the region of observation.

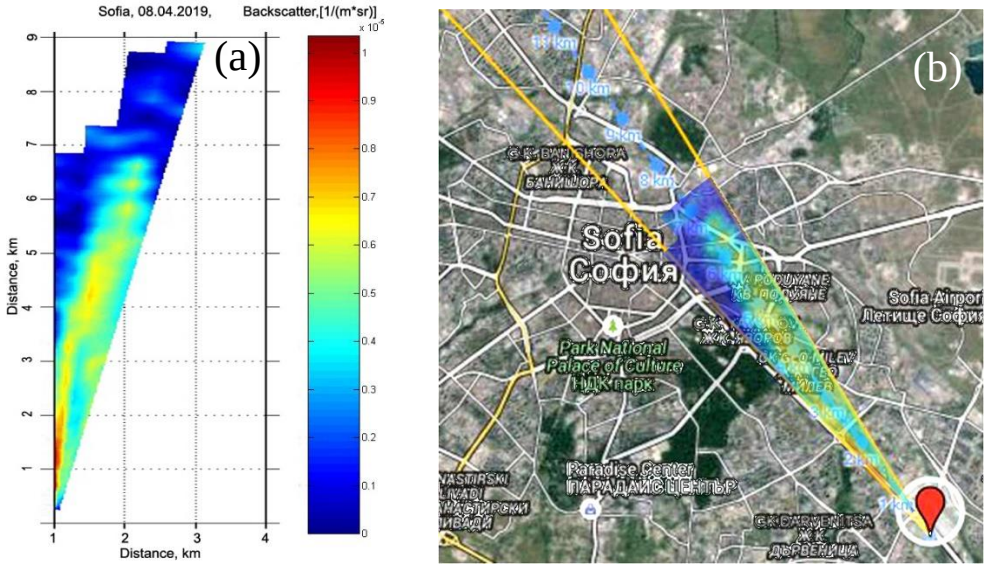

Fig. 5. Horizontal spatial distribution of the aerosol concentration around the direction toward the Sofia City Center above *Tsarigradsko Chaussee* blvd., measured on April 8, 2019 (a) and superimposed on the map of Sofia (b)

Conclusion

The results obtained in this work demonstrate the capabilities of the elastic lidar systems to probe rapidly the atmospheric aerosol fields on a large scale and with relatively high temporal and spatial resolutions. Two elastic-scatter lidar systems were employed to measure the spatial distribution of the aerosol backscatter (or extinction) coefficient over the vast areas of Sofia Valley. The dynamics of the backscatter coefficient distribution along a fixed LOS was also observed and analyzed. Thus, the possibility was illustrated to monitor the evolution of the aerosol fields as a whole. In addition, it was shown how, through appropriate calibration, one could transform the measured backscatter (extinction) coefficient distribution into aerosol mass-concentration distribution. The results from the elastic lidar sensing were presented as 2D horizontal diagrams and 3D diagrams of the backscatter-coefficient distribution superimposed on the maps of the region. Thus, “maps of the air pollution” were in fact created. As far as human health and ecosystems are concerned, most valuable are the results (horizontal 2D diagrams) describing the aerosol (PM) load distribution near the ground. Such regularly updated diagrams would timely indicate the cases of excessive air pollution and warn the city authorities of the need to take precautionary measures.

Acknowledgements

This work was carried out in the framework of the National Science Program "Environmental Protection and Reduction of Risks of Adverse Events and Natural Disasters", approved by the Resolution of the Council of Ministers № 577/17.08.2018 and supported by the Ministry of Education and Science (MES) of Bulgaria (Agreement № DO-230/06-12-2018).

References:

1. Fuzzi, S. et al., “Particulate matter, air quality and climate: lessons learned and future needs”, Atmos. Chem. Phys. 15, 8217–8299, 2015.
2. World Health Organisation (WHO). “Review of evidence on health aspects of air pollution-REVIHAAP Project”, Technical Report. Copenhagen, Denmark: WHO Regional Office for Europe, 2013.
3. Straif, K., A. Cohen, J. Samet, Eds., “Air Pollution and Cancer”. IARC Scientific Publication. Geneva, Switzerland: World Health Organisation, 2013.

4. Pappalardo, G. et al. “EARLINET: towards an advanced sustainable European aerosol lidar network”, Atmos. Meas. Tech. 7, 2389–2409, 2014.
5. He, T.-Y. et al., “Tracking of urban aerosols using combined LIDAR-based remote sensing and ground-based measurements”, Atmos. Meas. Tech. 5, 891–900, 2012.
6. Dreischuh, T., I. Grigorov, Z. Peshev, A. Deleva, G. Kolarov, D. Stoyanov, “Lidar Mapping of Near-Surface Aerosol Fields”, in: “Aerosols – Science and Case Studies”, K. Volkov, Ed., pp. 85-107, InTech (2016).
7. Measures, R.M., “Laser remote sensing”, New York: Wiley, 1984.
8. Klett, J., “Stable analytical inversion solution for processing lidar returns”, Appl Opt. 20, 211–220 (1981).
9. Fernald, F., “Analysis of atmospheric lidar observations: some comments”, Appl. Opt. 23, 652–653, 1984.
10. United States Committee on Extension to the Standard Atmosphere (COESA). U.S. Standard Atmosphere 1976. U.S. Government Printing Office, Washington, D.C. 1976. 241 p.
11. Mueller et al., “Aerosol-type-dependent lidar ratios observed with Raman lidar", Journal of Geophysical Research 112, D16202, 2007.
12. Wang, W., “Measurement and Study of Lidar Ratio by Usinga Raman Lidar in Central China”, Int. J. Environ. Res. Public Health,13, 508, 2016.
13. Ansmann, A. et al., “Ash and fine-mode particle mass profiles from EARLINET-AERONET observations over central Europe after the eruptions of the Eyjafjallajökull volcano in 2010”, J. Geophys. Res.-Atmos. 116, D20, 2011.
14. Angelova, R. et al., “Lidar and contact investigations of aerosol characteristics near high-traffic urban sites”, Proc. SPIE 1104713, 2019.
15. Directive 2008/50/EC of the European Parliament and of the Council of 21 May 2008 on ambient air quality and cleaner air for Europe.
16. Environmental Protection Act of Bulgaria, 2002(2017); https://www.moew.government.bg/en/environmental-protection-act-7628/